Splicing-dependent NMD requires Prp17 in *Saccharomyces cerevisiae*

Jikai Wen[1,2,3], Laetitia Marzi[1], Jianming Wang[1], Jinxin Ye[2], and Saverio Brogna[1]

1. School of Biosciences, University of Birmingham, Edgbaston, Birmingham, UK. B15 2TT

2. Guangdong Provincial Key Laboratory of Protein Function and Regulation in Agricultural Organisms, College of Life Sciences, South China Agricultural University, Tianhe District, Guangzhou, Guangdong 510642, P.R. China.

3. Key Laboratory of Zoonosis of Ministry of Agriculture, South China Agricultural University, Tianhe District, Guangzhou, Guangdong 510642, P.R. China

Abstract

Nonsense mediated mRNA decay (NMD) denotes that mutations, or errors in gene expression which introduce a premature translation termination codon (PTC), can decrease mRNA level in any organism. Remarkably, whether a PTC will lead to NMD often depends on the presence of a downstream intron, splicing of which marks a spliced mRNA by deposition of the exon junction complex (EJC) in mammalian cells. *Saccharomyces cerevisiae*, which has introns only in 5% of its genes and lacks proteins essential for the EJC assembly was not expected to undergo splicing-dependent NMD. Conversely, here we report that the presence of an intron can enhance NMD in a distance-dependent manner regardless of whether it is positioned before or after a PTC in this organism. Following screening for genes that might be specifically involved in splicing-dependent NMD, we identified splicing factor Prp17. Our data indicate that the coupling between splicing and translation is a universal feature of eukaryotes, and envisage that Prp17, which, notably, co-sediments with monosomal mRNA, may link splicing to NMD by bridging the spliceosome with the ribosome.

Running title: Splicing enhances NMD in *S. cerevisiae*

.

Introduction

Interrupting translation can greatly reduce mRNA levels in cells. The most apparent demonstration of this effect is the process of nonsense mediated mRNA decay (NMD). NMD occurs when nonsense or frameshift mutations or errors in transcription or pre-mRNA processing produce abnormal mRNAs encoding either a premature translation termination codon (PTC) or introduce other changes that place the normal stop codon in an atypical sequence context (Chang et al., 2007; Fatscher et al., 2015; He and Jacobson, 2015; Malabat et al., 2015; Muhlemann et al., 2008). NMD affects a large portion of a cell transcriptome and it is understood that, by destroying transcripts that could produce wasteful or toxic peptides, it might serve as a mechanism for increasing fidelity and efficiency of gene expression, and hence organism viability and development (Lykke-Andersen and Jensen, 2015; Muhlemann and Jensen, 2011). The consensus view is that NMD represents the functional output of an mRNA surveillance process that requires the concerted function of a core of evolutionary conserved proteins, including UPF1, UPF2 and UPF3, to discriminate and destroy mRNAs with a PTC or a PTC-like feature (He and Jacobson, 2015; Leeds et al., 1991); yet the molecular mechanism that would discriminate PTCs from normal stop codons remains unsatisfactorily understood in any organism (Brogna et al., 2016). It is in fact debatable whether cells have such a specialized mRNA decay pathway at all; NMD could in part be a passive consequence of ribosomes detaching prematurely, leaving the transcript unprotected by scanning ribosomes (Brogna et al., 2016).

Specifically, current models cannot fully explain the link between pre-mRNA splicing and NMD which has been observed in different organisms. Initial studies in human cells have concluded that a PTC induces strong NMD primarily when located upstream of an intron (Carter et al., 1996a; Thermann et al., 1998; Zhang and Maquat, 1996; Zhang et al., 1998). Although some later studies have downplayed this early view that NMD is strictly linked to splicing in mammalian cells (Buhler et al., 2006; Eberle et al., 2008; Silva et al., 2008; Singh et al., 2008), the presence of downstream introns remains a strong genome-wide predictor of whether a PTC will lead to NMD in mammalian cells (Hurt et al., 2013; Lindeboom et al., 2016; Mendell et al., 2004). Splice junctions are marked by the exon junction complex (EJC) - a multiprotein complex that binds mRNAs at splice junctions in the nucleus and remains associated with the mRNP until it is removed by the translating ribosome in the cytoplasm

(Le Hir et al., 2000a; Le Hir et al., 2000b; Le Hir et al., 2016). Therefore, current models predict that the presence of one or more downstream EJCs is what distinguishes PTCs from normal stop codons which, since they are typically located in the last exon, have no downstream EJCs (Maquat, 2004; Nagy and Maquat, 1998).

One study has reported that the EJC deposition might also enhance NMD in the evolutionarily distant organism *Neurospora crassa* (Zhang and Sachs, 2015). There are, however, examples of splicing-dependent NMD that the EJC model cannot explain (Brogna and Wen, 2009; Buhler et al., 2006; Carter et al., 1996b; Wang et al., 2002). Specifically, we have previously reported that splicing can enhance NMD in *Schizosaccharomyces pombe*, regardless of whether a PTC is located downstream or upstream of an exon-exon junction, and also in mutant strains lacking core EJC proteins (Wen and Brogna, 2010). These observations raise the possibility that there is a mechanism other than the EJC deposition that links splicing to NMD in *S. pombe*, and possibly other organisms.

S. cerevisiae is the first eukaryote in which NMD has been described (Losson and Lacroute, 1979); and extensively studied thereafter. Characteristically, only nonsense mutations that are close to the start of the coding region lead to strong NMD in this organism (Cao and Parker, 2003; Leeds et al., 1991; Losson and Lacroute, 1979; Peltz et al., 1993). The model is that PTCs further downstream do not induce NMD because they are sufficiently close to the normal 3'UTR to allow an interaction of poly(A) binding protein (PABPC) with the prematurely terminating ribosome which inhibits NMD (Amrani et al., 2004). However, the alternative possibility that PTCs at these positions do not cause NMD because there are no introns nearby has not been tested. Only a minority of protein coding genes contain introns in budding yeast - 285 out of 5749 based on a recent survey (Juneau et al., 2006); yet, these include ribosomal proteins and other highly expressed genes, hence pre-mRNA splicing is very efficient in this organism with more than 24% of the cellular mRNA estimated to be spliced (Ares et al., 1999; Juneau et al., 2006; Kupfer et al., 2004; Lin et al., 1985). Although *S. cerevisiae* genome does not encode Y14 and MAGO, proteins essential for the EJC assembly in mammalian cells (Le Hir et al., 2016), in view that splicing-dependent NMD does not require the EJC in *S. pombe*, we set to investigate whether splicing can also enhance NMD in this organism. Various gene-constructs were examined with an intron either upstream or downstream of a PTC and at different distances, and we screened for genes

that might specifically be involved in splicing-dependent NMD. Cumulatively, our data demonstrate that splicing can enhance NMD in *S. cerevisiae,* and thus, in contrast to current models, suggest that lack of a nearby intron is what prevents late PTCs from giving rise to strong NMD in this organism. Additionally, we provide evidence that splicing factor Prp17, which we find to co-sediment with ribosomal fractions, might be part of a novel mechanism that directly links splicing to translation and NMD.

Results

Splicing enhances NMD in *S. cerevisiae*

Initially, we assessed whether splicing affects NMD *in S. cerevisiae* by examining the expression of GFP NMD reporters with or without an intron (Fig 1A and Material and Methods). A PTC was introduced at codon positions 6 (PTC6) or 140 (PTC140); PTC6 being early in the coding region was expected to induce strong NMD based on previous observations, while PTC140, being in the second half of the ORF, should be much less effective in the absence of an intron (Kuperwasser et al., 2004; Wen and Brogna, 2010). Three introns, derived from the *ACT1*, *CYH2* and *UBC4* genes, were examined; all are efficiently spliced both *in vitro* and *in vivo* (Abelson et al., 2010; Lesser and Guthrie, 1993; Swida et al., 1986). The intron-containing reporters, in which the intron was inserted at codon position 110 (Fig 1A), are designated here by the suffixes A-*ivs*, C-*ivs* and U-*ivs*, carrying the *ACT1*, *CYH2* and *UBC4* introns respectively. All of the PTC-less reporters produced intense GFP fluorescence (Fig 1B), indicating that all introns are efficiently and correctly spliced. As expected, no fluorescence was detected in any of the strains transformed with the PTC-containing (PTC+) reporters. Bands of the size expected for spliced mRNAs were detected by Northern blotting (Fig 1C-1N). The pre-mRNA band is also visible in the A-*ivs* reporter, and C-*ivs* in particular, however, its intensity is weak relative to the spliced band. It is possible the introns are not spliced as efficiently in this sequence context as in the gene of origin. Both introns are close to the 5' end in the endogenous pre-mRNAs, and it has been reported that splicing becomes inefficient when introns are placed further downstream from the 5' end (Klinz and Gallwitz, 1985). In contrast, splicing of U-*ivs*, which is also close to the 5' end in the endogenous pre-mRNA, appears to be very efficient at this position, as we detected no pre-mRNA accumulation, consistent with the U-*ivs* intron being one of the most efficiently spliced introns *in vitro* (Abelson et al., 2010). U-*ivs* is 95 nt long (vs. A-*ivs* and C-*ivs* which are 309 nt and 501 nt, respectively); while such a slightly longer pre-mRNA band might be difficult to detect on the Northern blot, only the fragment corresponding to spliced transcript could be detected by RT-PCR. With respect to NMD, PTC6, as predicted, caused a strong mRNA reduction regardless of the presence of an intron (Fig 1C); in contrast, PTC140 induced strong NMD only in the reporters carrying either the A-*ivs* or C-*ivs* (Fig 1D and E). The shorter and apparently more efficiently spliced U-*ivs* intron

lead to a moderate NMD enhancement as the PTC140 mRNA level is reduced only to ~ 60% of that of the PTC-less control (Fig 1F vs. 1C). As expected, the relative levels of the PTC+ mRNAs are similar to those of the PTC-less controls in NMD mutant strains, *UPF2Δ* (Fig 1G-1J) and *UPF1Δ* strains (Fig 1K-1N). However, in some instances the levels of PTC+ mRNAs were increased above those of the PTC-less controls in the NMD mutants. This baffling effect has been reported previously in different organisms, and might result from nonspecific mRNA stabilization in NMD mutants (Brogna et al., 2016). We also examined several constructs in which the introns were inserted either in the 3'UTR of the GFP reporter or in the previously described PGK1-based intronless reporters (Peltz et al., 1993), nearby positions at which PTCs do not lead to NMD; however, at these locations all the introns tested are inactive or very inefficiently spliced, hence we could not reliably assess their effect on NMD (unpublished observations),

To examine the effect of splicing on NMD further, we generated additional reporters derived from two endogenous intron-containing genes, *CYH2* and *RPL11B* (Fig 2). In these, a PTC was introduced either downstream (*CYH2*) or upstream of the intron (*RPL11B*), and corresponding intron-less constructs were generated via cDNA cloning (Fig 2A). To allow detection of the transcripts by Northern blotting and to inhibit splicing-independent NMD at these otherwise early PTCs, a fragment of the *Drosophila melanogaster Adh* gene was inserted in frame at the start of the coding region of each gene. The presence of the PTC induced apparent NMD in both genes. The level of PTC+ mRNA was reduced down to ~29% (*CYH2*) and ~26% (*RPL11B*) relative to the corresponding PTC-less controls (Fig 2B, lanes 1-2 and 5-6). Instead, no evidence of NMD could be detected in the cDNA reporters lacking the intron (constructs labeled with the Δivs suffix, Fig 2B, lanes 3-4 and 7-8). Therefore, it appears that splicing can enhance NMD in these two genes as well and, as reported above for the GFP reporter, regardless of whether the PTC is located upstream (as in *RPL11B*) or downstream of the intron (as in *CYH2*). The levels of the PTC+ mRNAs are increased and comparable to that of the PTC-less controls in *UPF2Δ* (Fig 2C, lanes 1-2 and 5-6).

Next, we assessed whether the effect on NMD depends on the distance between an intron and a PTC. Two additional constructs were examined in which a spacer of either 147bp or 291bp was inserted at codon position 120 to lengthen the distance between the intron (at

position 110) and the NMD-inducing PTC at position 140 (Fig 3A). We found that the presence of a spacer clearly suppresses the ability of the intron to enhance NMD. The level of mRNA of the initial reporter without a spacer (PTC140-Aivs) was ~27% of the PTC-less control (Fig 3B, lanes 1-2). In contrast, neither of the spacer-containing constructs undergo NMD: the mRNA level of the shorter spacer (PTC140-Aivs-147) was 96% of the PTC- control, while it was ~110% of the longer spacer (PTC140-Aivs-291). The results indicate that an intron must be relatively close to a PTC for splicing to enhance NMD. The distance between the intron and the PTC was 90 nt in the NMD-sensitive construct, while it was 243 nt and 387 nt in the two longer constructs (Fig 3B).

Prp17 is required for splicing-dependent NMD and co-fractionates with monosomes

To gain insight into what the mechanism that links splicing to NMD might be, we screened 33 viable *S. cerevisiae* strains containing deletions in known or predicted splicing factors as well as proteins predicted to interact with one of the upf proteins. These were tested along the three known upf deletion strains; all were isolated from the commercially available Yeast MATalpha collection (Supplementary Table 3 and Material and Methods). The strains were blindly relabeled and transformed with a centromeric plasmid construct expressing GFP with or without a PTC or C-*ivs* intron (Fig 4A). The intron-less reporters carrying PTC6 were used to examine splicing-independent NMD, while PTC140-C*ivs* was used as a reporter of splicing-dependent NMD. By means of Northern blotting we identified six strains with an apparent NMD-suppression phenotype. Three of these correspond to *UPF1Δ*, *UPF2Δ* and *UPF3Δ*, as expected (Fig. 4 B-E); the others were deletions of *PRP17*, *CWC21* and *LSM6* (Fig. 4 F-H). Although the level of spliced mRNA is, as expected, lower than that of the intron-less reporter in some of the mutants, clearly, the presence of PTC140 does not reduce its level to the extent that it does in wild-type; thus indicating NMD suppression in these mutants. A similar NMD suppression phenotype was seen with the intron-less PTC6 reporter in all but one mutant. The exception was *PRP17Δ*, in which the level of the spliced PTC140 mRNA was comparable to the PTC-less control, while that of PTC6 was clearly unaffected, showing as strong NMD as in the wild-type strain (Fig 4F, lanes 3-4 vs. 1-2). Similar constructs carrying the A-*ivs* intron instead of C-*ivs* were also tested. Their analysis revealed similar mRNA expression patterns; both splicing-dependent and splicing-independent NMD was suppressed in *UPF1Δ* and *CWC21Δ* but, as shown above, in *PRP17Δ* only the level of the

spliced PTC140 mRNA was increased (Supplementary Fig 1). The interpretation is that Prp17 might be selectively involved in linking splicing to NMD.

As NMD strictly depends on translation, we examined whether Prp17 associates with ribosomal fractions. Following standard whole-cell sucrose gradient fractionation, we found that a portion of GFP-tagged Prp17 co-sediments with ribosomal subunits and monosomes, and to a smaller extent, polysomes (Fig 5B); such distribution patterns parallel those of similarly tagged Upf1 and Upf2 (Fig 5C and 5D) but differ from those of Upf3p-GFP, which are also apparent in polysomal fractions (Fig 5E). Cwc21-GFP was instead detected only in lighter sub-ribosomal fractions, as expected (Supplementary Fig 5F). Although we cannot exclude that sedimentation of Prp17 and other proteins examined is partially affected by GFP tagging, the data indicate that a fraction of Prp17 might associate with actively translated mRNA or ribosomal subunits directly.

Finally, we considered whether the enhancing effect of splicing on NMD might be an indirect consequence of increased translation efficiency of spliced mRNA. We generated reporters in which the firefly luciferase coding sequence was fused to that of GFP, which was either intron-less or carrying A*ivs* or C*ivs* (Fig 6A). Level of mRNA and luciferase were quantified in parallel to estimate translation yield (Fig 6B-C). We found that the spliced mRNA deriving from reporter containing the A-*ivs* intron appears to be translated more efficiently in wild type and some of the mutant strains, yet translation yield of the construct with the C-*ivs* intron, which similarly enhanced NMD, increased only slightly in wild type and is reduced in some of the mutants (Fig 6C). Therefore, while spliced mRNA might be translated more efficiently in wild-type and some of the mutant strains to a variable extent, the effect does not correlate with either the extent of NMD or its suppression in the mutants. Specifically, translation yield in *PRP17Δ* is clearly similar between intron-containing and intron-less reporters and comparable to that in wild-type (Fig 6C).

Discussion

As discussed, only nonsense mutations at the beginning of the gene lead to apparent NMD in *S. cerevisiae,* such polarity is not typically seen, or it is limited to the 3' terminal exon, in mammalian cells (Eberle et al., 2008). Lack of polarity is linked to the presence of one or more introns downstream of a PTC which, via deposition of the EJC, is understood to trigger NMD regardless of the distance of the PTC from either end of the transcript in mammalian cells (Maquat, 2004). There is no evidence of an EJC in *S. cerevisiae*, and out of the few genes that have introns (~5%), the vast majority (~97%) contain a single intron located very close to the start of the coding region (Schreiber et al., 2015). It was therefore envisaged that there would not be any mechanism linking splicing and NMD in this organism. On the contrary, here we have shown that inserting an intron in a gene harboring a late PTC causes apparent NMD in *S. cerevisiae* as well. We examined constructs with different introns, either upstream or downstream of a PTC and at different distances, and found that an intron can enhance NMD regardless of whether it is located before or after the PTC. One determinant of strong NMD appears to be the vicinity of the intron to the PTC, while another might be intron length. Of the three introns we examined, the most effective at enhancing NMD were the long *ACT1* and *CYH2* introns, whereas the least effective was the shortest *UBC4* intron. This set of observations is similar to what has been reported in *S. pombe* (Wen and Brogna, 2010); it is also consistent with the report that splicing-dependent NMD appears to be independent of EJC deposition in the protozoan Tetrahymena (Tian Miao, 2017); and indicates that all eukaryotes have mechanism(s) linking splicing to translation and NMD.

The outstanding question is how these mechanism(s) operate. The lack of Y14 and MAGO homologues in *S. cerevisiae* makes it unlikely that an EJC-like complex can be assembled at splice junctions, for example by stabilization of eIF4AIII binding on mRNA via protein interactions other than those described for the EJC in mammalian cells (Ballut et al., 2005). Moreover, eIF4AIII is likely to bind nascent RNA independently of splicing in yeast, as it has been reported for *Drosophila* (Choudhury et al., 2016). It is conceivable that Prp17 is directing deposition of an EJC-like but molecular distinct complex, which, by remaining on the mRNA during nuclear export, could affect translation and NMD in the cytoplasm. The co-sedimentation of Prp17 with ribosomal fractions and monosomes, would seem consistent with this view as it indicates that this protein can interact with the ribosome as well as the

spliceosome (Zhang et al., 2017). Additionally, monosomal mRNAs appear to be more sensitive to NMD in *S. cerevisiae* (Heyer and Moore, 2016). However, it is difficult to explain our observations with any EJC-like tagging model because an intron can also enhance NMD when located upstream of the PTC, and any complex associated with the exon junction will have to be removed by the ribosome before reaching the PTC (Qin et al., 2014; Yusupova et al., 2001).

Although, the NMD suppression phenotype of some of the splicing factors deletion strains we have identified might be in part indirect, that of Prp17 appears to be direct as it is specifically required for splicing-dependent NMD. Prp17 is thought to be involved in the second step of splicing (Jones et al., 1995; Will and Luhrmann, 2011); possibly of introns which, like those of *ACT1* and *CYH2,* are longer than average based on some studies (Clark et al., 2002; Kawashima et al., 2009; Sapra et al., 2004). It is possible that the effect of the other two mutants is indirect. For example, Lsm6, as other SM-like proteins, were reported to function in general mRNA decapping and decay, so the NMD suppression we observed could be a consequence of inhibiting global mRNA turnover which results in some transcripts being affected more than others (Tharun et al., 2000). Perhaps a similar effect occurs in *CWC21Δ*; Cwc21, although not essential, is likely to have a global effect on splicing, which would also result in indirect global transcriptomic changes (Khanna et al., 2009).

In summary, our data demonstrate that splicing can also enhance NMD in *S. cerevisiae* and suggest that lack of nearby introns is a factor that stops late PTCs from causing strong NMD in this organism, and perhaps the evolutionary drive for why introns are rare in 3'UTRs in organisms with intron-rich genomes (Hong et al., 2006). As for the mechanism that couples splicing with NMD, we discussed that the effect is unlikely to be a consequence of splicing changing conformation and composition of the mRNP which is exported to the cytoplasm, as postulated by the EJC or other models built on the observation that splicing factors can shuttle from the nucleus to the cytoplasm (Sanford et al., 2004). Instead, the data suggest that Prp17 might directly link splicing to NMD by bridging the spliceosome with the ribosome .

Materials and Methods

Plasmids and strains

GFP-based NMD reporters were generated by cloning the coding sequence of the S65T GFP variant (accession number BD062761) into the BamHI sites of either pRS416 or pRS304 vector, flanked by TDH3 promoter and terminator sequences (Kuperwasser et al., 2004). Mutations were introduced by overlapping PCR and verified by sequencing. The intron of the pGFP-ivs construct derives from ACT1*, CYH2* or *UBC4* gene, which were all amplified from *S. cerevisiae* genomic DNA and cloned into the PmlI site at position 328 in the coding region (codon 110, out of frame) by blunt-end ligation. The pGFP-A*ivs*-147 and pGFP-A*ivs*-291 constructs were generated by inserting either a 147 or 291 bp DNA fragment in the AvrII site by overlapping PCR; AvrII site is 34 bp downstream of the *ACT1* intron. The fragments correspond to overlapping regions of the firefly luciferase gene (see primer sequences in Supplementary). The *RpL11B* and the *CYH2* genes were amplified from yeast genomic DNA or cDNA while the nonsense mutations were introduced by overlapping PCR and then cloned into pRS304-*Dm*ADH (see primer sequences). Unless otherwise indicated, the strains were isolated from the available Yeast MATalpha Collection (YSC1054). The strains are listed in Supplementary Table 1 and primers in Supplementary Table 2.

Yeast transformation

Transformations were performed using the lithium acetate method as previously described (Soni et al., 1993), with minor modifications. In brief, 100 μL of yeast cell pellet (about 10^8 cells per transformation) was resuspended and vigorously vortexed in 360 μL of freshly prepared transformation mix (33% PEG 3350, 100 μg ssDNA, 500 ng plasmid DNA in 0.1 M LiAc), incubated at 30^0C for 20 minutes, and then heat shocked at 42^0C in a water bath for 45 minutes. After heat shock, the yeast cells were pelleted by centrifugation, at 5000 rpm for 1 min, washed once with 1 mL of sterile water, resuspended in 1 mL of the same and 1/10 to 1/5 of it was spread on the selective Synthetic Drop-out Media plate (Formedium, UK). The plates were typically incubated at 30^0C for 2 days until transformants colonies reached up to 0.5 mm in diameter.

Northern blot assay

Total RNA was typically extracted from 10 mL cell cultures grown to 1-2 OD_{600}, using hot acid phenol method as described (Ausubel et al., 1996). RNA was separated on 1.2% agarose gels in the presence of formaldehyde. RNA was blotted overnight by capillary transfer onto a nylon membrane (Hybond-N, GE Healthcare) and hybridized with ^{32}P random primed labelled probes as described (Yang et al., 1993). Probes were PCR amplified from plasmid clones (*GFP* and *DmADH*) or from genomic DNA (*rpL32*). Radioactive membranes were imaged using a phosphorimager (Molecular Image™-FX, Bio-Rad), and the intensity of bands calculated using the Quantity One software (Bio-Rad).

Luciferase assay

Yeast culture densities were adjusted to 1 OD_{600}. Then, 10 μL of each culture was mixed with 15 μL of sterile purified water and loaded onto a 96-well microtiter plate which contained 25 μL of Steady-Glo luciferase substrate solution (Promega) in each well. Chemiluminescence was measured in triplicates of each culture using a microplate reader (Tecan). Relative GFP mRNA levels were quantified by real-time qRT-PCR with primers spanning the exons junction specific for the spliced transcript (GFP.Qs.rev and GFP.Q.fow, Supplementary Table 2), from equal amounts of total-RNA.

Polyribosome profile

100 mL of yeast cell cultures were grown to 0.8 OD_{600} and pretreated (15 min) with 100 μg/mL cycloheximide, pelleted by centrifugation at 4°C and then washed once in wash buffer (20 mM HEPES pH 7.4, 2 mM magnesium acetate, 2 mM $MgCl_2$, 100 mM potassium acetate, 1 mM dithiothreitol (DTT)). Yeast cells were pelleted again, and resuspended in 300 μL lysis buffer - 20 mM HEPES pH 7.4, 2 mM magnesium acetate, 2 mM $MgCl_2$, 100 mM potassium acetate, 1 mM DTT, 250 μg/mL heparin, 20 units/mL of RiboLock RNase inhibitor (Fermentas), 0.6% Triton X-100, 100 μg/mL cycloheximide, EDTA free Complete Protease Inhibitor Cocktail (Roche), and 1mM phenylmethanesulfonyl fluoride (PMSF). The cells were lysed by shaking using 500 mg of glass beads (0.5 mm, Sigma) in a Precellys 24 homogenizer (Bertin Corp.). Cell lysates were cleared of nuclei, mitochondria and insoluble cell debris by centrifugation at maximum speed for 20 min in a microcentrifuge at 4°C. Typically 40 OD_{260}

units of extracts blanked with lysis buffer were loaded on 11 mL of a linear 10%–50% sucrose gradient (prepared in 20 mM HEPES pH 7.4, 2 mM magnesium acetate, 2 mM $MgCl_2$, 100 mM potassium acetate) and centrifuged at 38,000 rpm for 2 h and 40 min in a SW40Ti rotor (Beckman). After centrifugation, fractions (typically 0.9 mL) were recovered from the bottom of the tube using a capillary cannula attached to a peristaltic pump and absorbance was monitored during fractionation using a UV monitor with flow-cell equipped with a 254-nm filter (UA-6, Teledyne ISCO). Fractions were precipitated by adding 1/10 volume of 100% trichloroacetic acid (TCA), vortexing, over-night incubation at 4°C which was followed by centrifugation at maximum speed for 30 min in a microfuge. The supernatant was then carefully removed and the precipitate was washed twice in ice-cold acetone and centrifuged for 2 min at 4°C; the pellet was analyzed by standard SDS-PAGE and Western blotting using anti-GFP polyclonal antibody (AbD Serotec).

Acknowledgments

We thank Stephen Dove for help and support, and Michael Rosbash, He Feng, Alan Jacobson and Jean D. Beggs for providing reagents. We also thank Marija Petric and Anand Singh for critically reading the manuscript. This work was supported by the Wellcome Trust (9340/Z/09/Z) and BBSRC (BB/M022757/1) project grants to SB, and a grant from National Natural Science Foundation of China (NSFC, Grant No. 34171234) to JW.

Contributions

Saverio Brogna (SB) and Jikai Wen (JW) conceived the study. JW performed most of the experiments. JW and Laetitia Marzi performed the mutants screening, JW and Jianming Wang performed the polysomal fractionation. Jinxin Ye made some of the mutant strains. SB and JW wrote the paper.

Competing financial interests

The authors declare no competing financial interests.

References

Abelson, J., Blanco, M., Ditzler, M.A., Fuller, F., Aravamudhan, P., Wood, M., Villa, T., Ryan, D.E., Pleiss, J.A., Maeder, C*., et al.* (2010). Conformational dynamics of single pre-mRNA molecules during in vitro splicing. Nature structural & molecular biology *17*, 504-512.

Amrani, N., Ganesan, R., Kervestin, S., Mangus, D.A., Ghosh, S., and Jacobson, A. (2004). A faux 3'-UTR promotes aberrant termination and triggers nonsense-mediated mRNA decay. Nature *432*, 112-118.

Ares, M., Grate, L., and Pauling, M.H. (1999). A handful of intron-containing genes produces the lion's share of yeast mRNA. Rna-a Publication of the Rna Society *5*, 1138-1139.

Ausubel, F.A., Brent, R., Kingston, R.E., Moore, D.D., Seidman, J.G., Smith, J.A., and K., S. (1996). Current Protocols in Molecular Biology. (New York: John Wiley & Sons).

Ballut, L., Marchadier, B., Baguet, A., Tomasetto, C., Seraphin, B., and Le Hir, H. (2005). The exon junction core complex is locked onto RNA by inhibition of eIF4AIII ATPase activity. Nat Struct Mol Biol *12*, 861-869.

Brogna, S., McLeod, T., and Petric, M. (2016). The Meaning of NMD: Translate or Perish. Trends Genet *32*, 395-407.

Brogna, S., and Wen, J. (2009). Nonsense-mediated mRNA decay (NMD) mechanisms. Nat Struct Mol Biol *16*, 107-113.

Buhler, M., Steiner, S., Mohn, F., Paillusson, A., and Muhlemann, O. (2006). EJC-independent degradation of nonsense immunoglobulin-mu mRNA depends on 3' UTR length. Nat Struct Mol Biol *13*, 462-464.

Cao, D., and Parker, R. (2003). Computational modeling and experimental analysis of nonsense-mediated decay in yeast. Cell *113*, 533-545.

Carter, M.S., Li, S., and Wilkinson, M.F. (1996a). A splicing-dependent regulatory mechanism that detects translation signals. The EMBO journal *15*, 5965-5975.

Carter, M.S., Li, S.L., and Wilkinson, M.F. (1996b). A splicing dependent regulatory mechanism that detects translation signals. Embo J *15*, 5965-5975.

Chang, Y.F., Imam, J.S., and Wilkinson, M.F. (2007). The nonsense-mediated decay RNA surveillance pathway. Annu Rev Biochem *76*, 51-74.

Choudhury, S.R., Singh, A.K., McLeod, T., Blanchette, M., Jang, B.Y., Badenhorst, P., Kanhere, A., and Brogna, S. (2016). Exon junction complex proteins bind nascent transcripts independently of pre-mRNA splicing in Drosophila melanogaster. Elife *5*.

Clark, T.A., Sugnet, C.W., and Ares, M. (2002). Genomewide analysis of mRNA processing in yeast using splicing-specific microarrays. Science *296*, 907-910.

Eberle, A.B., Stalder, L., Mathys, H., Orozco, R.Z., and Muhlemann, O. (2008). Posttranscriptional gene regulation by spatial rearrangement of the 3' untranslated region. PLoS Biol *6*, e92.

Fatscher, T., Boehm, V., and Gehring, N.H. (2015). Mechanism, factors, and physiological role of nonsense-mediated mRNA decay. Cell Mol Life Sci *72*, 4523-4544.

He, F., and Jacobson, A. (2015). Nonsense-Mediated mRNA Decay: Degradation of Defective Transcripts Is Only Part of the Story. Annu Rev Genet.

Heyer, E.E., and Moore, M.J. (2016). Redefining the Translational Status of 80S Monosomes. Cell *164*, 757-769.

Hong, X., Scofield, D.G., and Lynch, M. (2006). Intron size, abundance, and distribution within untranslated regions of genes. Mol Biol Evol *23*, 2392-2404.

Hurt, J.A., Robertson, A.D., and Burge, C.B. (2013). Global analyses of UPF1 binding and function reveal expanded scope of nonsense-mediated mRNA decay. Genome Res *23*, 1636-1650.

Jones, M.H., Frank, D.N., and Guthrie, C. (1995). Characterization and functional ordering of Slu7p and Prp17p during the second step of pre-mRNA splicing in yeast. Proc Natl Acad Sci U S A *92*, 9687-9691.

Juneau, K., Miranda, M., Hillenmeyer, M.E., Nislow, C., and Davis, R.W. (2006). Introns regulate RNA and protein abundance in yeast. Genetics *174*, 511-518.

Kawashima, T., Pellegrini, M., and Chanfreau, G.F. (2009). Nonsense-mediated mRNA decay mutes the splicing defects of spliceosome component mutations. Rna-a Publication of the Rna Society *15*, 2236-2247.

Khanna, M., Van Bakel, H., Tang, X.Y., Calarco, J.A., Babak, T., Guo, G., Emili, A., Greenblatt, J.F., Hughes, T.R., Krogan, N.J.*, et al.* (2009). A systematic characterization of Cwc21, the yeast ortholog of the human spliceosomal protein SRm300. Rna-a Publication of the Rna Society *15*, 2174-2185.

Klinz, F.J., and Gallwitz, D. (1985). Size and position of intervening sequences are critical for the splicing efficiency of pre-mRNA in the yeast Saccharomyces cerevisiae. Nucleic Acids Res *13*, 3791-3804.

Kuperwasser, N., Brogna, S., Dower, K., and Rosbash, M. (2004). Nonsense-mediated decay does not occur within the yeast nucleus. RNA *10*, 1907-1915.

Kupfer, D.M., Drabenstot, S.D., Buchanan, K.L., Lai, H.S., Zhu, H., Dyer, D.W., Roe, B.A., and Murphy, J.W. (2004). Introns and splicing elements of five diverse fungi. Eukaryot Cell *3*, 1088-1100.

Le Hir, H., Izaurralde, E., Maquat, L.E., and Moore, M.J. (2000a). The spliceosome deposits multiple proteins 20-24 nucleotides upstream of mRNA exon-exon junctions. Embo J *19*, 6860-6869.

Le Hir, H., Moore, M.J., and Maquat, L.E. (2000b). Pre-mRNA splicing alters mRNP composition: evidence for stable association of proteins at exon-exon junctions. Genes Dev *14*, 1098-1108.

Le Hir, H., Sauliere, J., and Wang, Z. (2016). The exon junction complex as a node of post-transcriptional networks. Nat Rev Mol Cell Biol *17*, 41-54.

Leeds, P., Peltz, S.W., Jacobson, A., and Culbertson, M.R. (1991). The product of the yeast Upf1 gene is required for rapid turnover of messenger RNAs containing a premature translational termination codon. Genes & development *5*, 2303-2314.

Lesser, C.F., and Guthrie, C. (1993). Mutational analysis of pre-mRNA splicing in Saccharomyces cerevisiae using a sensitive new reporter gene, CUP1. Genetics *133*, 851-863.

Lin, R.J., Newman, A.J., Cheng, S.C., and Abelson, J. (1985). Yeast mRNA splicing in vitro. J Biol Chem *260*, 14780-14792.

Lindeboom, R.G.H., Supek, F., and Lehner, B. (2016). The rules and impact of nonsense-mediated mRNA decay in human cancers. Nature Genetics *48*, 1112-1118.

Losson, R., and Lacroute, F. (1979). Interference of nonsense mutations with eukaryotic messanger RNA stability. Proc Natl Acad Sci USA *76*, 5134-5137.

Lykke-Andersen, S., and Jensen, T.H. (2015). Nonsense-mediated mRNA decay: an intricate machinery that shapes transcriptomes. Nat Rev Mol Cell Biol *16*, 665-677.

Malabat, C., Feuerbach, F., Ma, L., Saveanu, C., and Jacquier, A. (2015). Quality control of transcription start site selection by nonsense-mediated-mRNA decay. Elife *4*.

Maquat, L.E. (2004). Nonsense-mediated mRNA decay: splicing, translation and mRNP dynamics. Nat Rev Mol Cell Biol *5*, 89-99.

Mendell, J.T., Sharifi, N.A., Meyers, J.L., Martinez-Murillo, F., and Dietz, H.C. (2004). Nonsense surveillance regulates expression of diverse classes of mammalian transcripts and mutes genomic noise. Nat Genet *36*, 1073-1078.

Muhlemann, O., Eberle, A.B., Stalder, L., and Zamudio Orozco, R. (2008). Recognition and elimination of nonsense mRNA. Biochimica et Biophysica Acta (BBA) - Gene Regulatory Mechanisms *1779*, 538-549.

Muhlemann, O., and Jensen, T.H. (2011). mRNP quality control goes regulatory. Trends Genet *28*, 70-77.

Nagy, E., and Maquat, L.E. (1998). A rule for termination-codon position within intron-containing genes: when nonsense affects RNA abundance. Trends Biochem Sci *23*, 198-199.

Peltz, S.W., Brown, A.H., and Jacobson, A. (1993). Messenger RNA destabilization triggered by premature translational termination depends on at least 3 cis-acting sequence elements and one trans-acting factor. Genes & development *7*, 1737-1754.

Qin, P.W., Yu, D.M., Zuo, X.B., and Cornish, P.V. (2014). Structured mRNA induces the ribosome into a hyper-rotated state. EMBO reports *15*, 185-190.

Sanford, J.R., Gray, N.K., Beckmann, K., and Caceres, J.F. (2004). A novel role for shuttling SR proteins in mRNA translation. Genes Dev *18*, 755-768.

Sapra, A.K., Arava, Y., Khandelia, P., and Vijayraghavan, U. (2004). Genome-wide analysis of Pre-mRNA splicing - Intron features govern the requirement for the second-step factor, Prp17 in Saccharomyces cerevisiae and Schizosaccharomyces pombe. Journal of Biological Chemistry *279*, 52437-52446.

Schreiber, K., Csaba, G., Haslbeck, M., and Zimmer, R. (2015). Alternative Splicing in Next Generation Sequencing Data of Saccharomyces cerevisiae. Plos One *10*.

Silva, A.L., Ribeiro, P., Inacio, A., Liebhaber, S.A., and Romao, L. (2008). Proximity of the poly(A)-binding protein to a premature termination codon inhibits mammalian nonsense-mediated mRNA decay. RNA *14*, 563-576.

Singh, G., Rebbapragada, I., and Lykke-Andersen, J. (2008). A competition between stimulators and antagonists of Upf complex recruitment governs human nonsense-mediated mRNA decay. PLoS Biol *6*, e111.

Soni, R., Carmichael, J.P., and Murray, J.A. (1993). Parameters affecting lithium acetate-mediated transformation of Saccharomyces cerevisiae and development of a rapid and simplified procedure. Curr Genet *24*, 455-459.

Swida, U., Thuroff, E., and Kaufer, N.F. (1986). Intron mutations that affect the splicing efficiency of the CYH2 gene of Saccharomyces cerevisiae. Molecular & general genetics : MGG *203*, 300-304.

Tharun, S., He, W.H., Mayes, A.E., Lennertz, P., Beggs, J.D., and Parker, R. (2000). Yeast Sm-like proteins function in mRNA decapping and decay. Nature *404*, 515-518.

Thermann, R., NeuYilik, G., Deters, A., Frede, U., Wehr, K., Hagemeier, C., Hentze, M.W., and Kulozik, A.E. (1998). Binary specification of nonsense codons by splicing and cytoplasmic translation. Embo J *17*, 3484-3494.

Tian Miao, W.Y., Jing Zhang, Huai Dang, Xingyi Lu, Chengjie Fu, Miao Wei (2017). Nonsense-mediated mRNA decay in Tetrahymena is EJC independent and requires a protozoa-specific nuclease. Nucleic Acids Res *gkx256*.

Wang, J., Gudikote, J.P., Olivas, O.R., and Wilkinson, M.F. (2002). Boundary-independent polar nonsense-mediated decay. EMBO reports *3*, 274-279.

Wen, J., and Brogna, S. (2010). Splicing-dependent NMD does not require the EJC in Schizosaccharomyces pombe. The Embo Journal *29*, 1537-1551.

Will, C.L., and Luhrmann, R. (2011). Spliceosome structure and function. Cold Spring Harb Perspect Biol *3*.

Yang, H., McLeese, J., Weisbart, M., Dionne, J.L., Lemaire, I., and Aubin, R.A. (1993). Simplified high throughput protocol for northern hybridization. Nucleic Acids Res *21*, 3337-3338.

Yusupova, G.Z., Yusupov, M.M., Cate, J.H., and Noller, H.F. (2001). The path of messenger RNA through the ribosome. Cell *106*, 233-241.

Zhang, J., and Maquat, L.E. (1996). Evidence that the decay of nucleus-associated nonsense mRNA for human triosephosphate isomerase involves nonsense codon recognition after splicing. RNA *2*, 235-243.

Zhang, J., Sun, X., Qian, Y., LaDuca, J.P., and Maquat, L.E. (1998). At least one intron is required for the nonsense-mediated decay of triosephosphate isomerase mRNA: a possible link between nuclear splicing and cytoplasmic translation. Mol Cell Biol *18*, 5272-5283.

Zhang, X.F., Yan, C.Y., Hang, J., Finci, L.I., Lei, J.L., and Shi, Y.G. (2017). An Atomic Structure of the Human Spliceosome. Cell *169*, 918-+.

Zhang, Y., and Sachs, M.S. (2015). Control of mRNA Stability in Fungi by NMD, EJC and CBC Factors Through 3'UTR Introns. Genetics *200*, 1133-1148.

Figure Legends

Figure 1. Splicing enhanced NMD in *S. cerevisiae*.

(A) Schematic maps of NMD reporters. The GFP gene was cloned into pRS304, which is regulated by promoter and terminator of *S. cerevisiae TDH3* gene. The schematic of the intron-less constructs is on top, while below is that of the intron-containing constructs containing one of the three *S. cerevisiae* introns, labeled *ivs* ; A-*ivs*, C-*ivs* and U-*ivs* which derive from the *ACT1*, *CYH2* and *UBC4* genes, respectively. (B) From left to right panel – micrographs showing GFP fluorescence of cells transformed with indicated reporters; the right panel shows a PTC+ control not expected to produce GFP fluorescence. Images were taken with an inverted fluorescence microscope (Nikon Ti). (C-F) Northern blot analysis of mRNA levels in cells transformed with the indicated NMD reporters. Top panels show hybridization of a GFP-specific probe, the bottom panel shows a probe specific for the ribosomal protein L32 mRNA (Rpl32), as a loading control. The values below each lane are percentages with standard variations of the level of GFP mRNA relative to that of the corresponding PTC-less control, lane 1 in each panel. Bands intensities were quantified using a phophorimager and divided by the RpL32 band intensity in the same blot (see Materials and methods). (G-H) Similar Northern blot analysis carried out in *UPF2Δ* and (K-N) *UPF1Δ.* All of the experiments were repeated three times.

Figure 2. The splicing enhanced NMD is observed in endogenous genes.

(A) Schematic maps of NMD reporters expressing two endogenous intron-containing genes, *CYH2* and *RpL11B*, and corresponding cDNA derivatives lacking the intron. A DNA fragment from *Drosophila melanogaster Adh* gene (*DmA*) was fused to the 5'end of the constructs to allow detection by Northern blotting. (B) Northern blotting detection of CYH2 (top left panel) and RPL11B transcripts (top right panel); corresponding bottom panels show RpL32 mRNA (C). Similar analysis as above in *UPF2Δ*. All of the experiments were repeated three times.

Figure 3. Lengthening the distance between an intron and a PTC abolishes splicing-dependent NMD.

(A) Schematic maps of NMD reporters carrying different spacer inserts between PTC140 and the intron. The two spacers, 147 bp and 291 bp, were inserted at codon position 120. (B) Northern blotting analysis of GFP transcripts (top panel); the bottom panel shows the *Rpl32*

signal used as a loading control. (C) Same as in B in *UPF2Δ* transformants. All of the experiments were repeated three times.

Figure 4. Deletion of Prp17 specifically suppresses splicing-dependent NMD.

(A) Schematic maps of the gene reporters used in the screening for splicing and other factors that might be involved in NMD. (B-H) Northern blot analysis of the reporters expression carried out in wild type (*BY4742)* (B), *UPF1Δ* (C), *UPF2Δ* (D), *UPF3Δ* (E), *PRP17Δ* (F), *CWC21Δ* (G) and *LSM6Δ* (H). Top panels show GFP hybridization signal; the bottom panels show those of the normalization control *Rpl32B* mRNA. All the experiments were repeated three times.

Figure 5. Prp17 co-sediments with ribosomal fractions.

(A) Western blotting of strains expressing Prp17 and other indicated GFP-tagged proteins, using an anti-GFP polyclonal antibody. (B) Absorbance profile (OD_{254}) following sucrose gradient sedimentation of the whole-cell extract from a strain expressing Prp17-GFP. Fractions containing 40S, 60S, 80S and polysomes are labeled. The panel below shows Western blotting of the whole protein-extract from each fraction using the GFP antibody. (C-F) Similar experiments using strains expressing GFP-tagged Upf1 (C), Upf2 (D), Upf3 (E) and Cwc21 (F).

Figure 6. Introns have variable effects on translation yield.

(A) Diagram of the GFP reporters: intronless GFP (top), GFP split with either *ACT1* or *CYH2* intron (below), both fused with firefly luciferase at the carboxyl terminal. (B). The three plasmid constructs were transformed into wild type or *UPF1Δ*, *UPF2Δ*, *UPF3Δ*, *PRP17Δ*, *CWC21Δ* or *LSM6Δ*. Relative levels of GFP mRNA were quantified by qRT-PCR using primers spanning the exons junction specific for the spliced transcript, from equal amounts of total-RNA (see Material and Methods). Quantifications are based on three separate experiments. (C) Luciferase activities measured in aliquots of the same cultures used for the mRNA quantification in B. Luciferase relative light units were normalized to mRNA levels and are shown as means of three measurements with standard deviations.

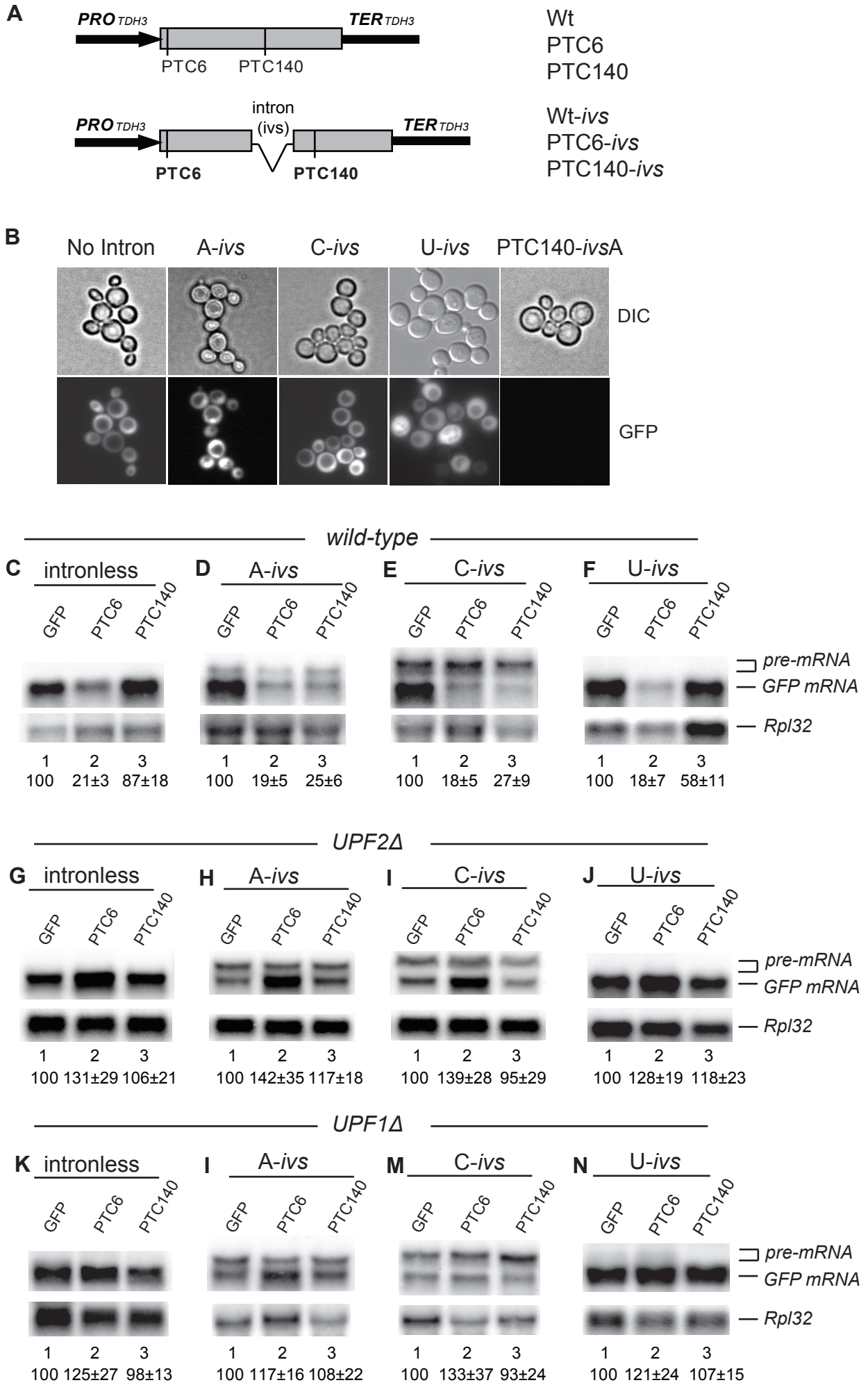
A
PRO TDH3
TER TDH3
PTC6
PTC140
Wt
PTC6
PTC140
intron
(ivs)
Wt-ivs
PTC6-ivs
PTC140-ivs
B
No Intron
A-ivs
C-ivs
U-ivs
PTC140-ivsA
DIC
GFP
wild-type
C intronless
D A-ivs
E C-ivs
F U-ivs
GFP
PTC6
PTC140
pre-mRNA
GFP mRNA
Rpl32
1 2 3
100 21±3 87±18
100 19±5 25±6
100 18±5 27±9
100 18±7 58±11
UPF2Δ
G intronless
H A-ivs
I C-ivs
J U-ivs
100 131±29 106±21
100 142±35 117±18
100 139±28 95±29
100 128±19 118±23
UPF1Δ
K intronless
I A-ivs
M C-ivs
N U-ivs
100 125±27 98±13
100 117±16 108±22
100 133±37 93±24
100 121±24 107±15

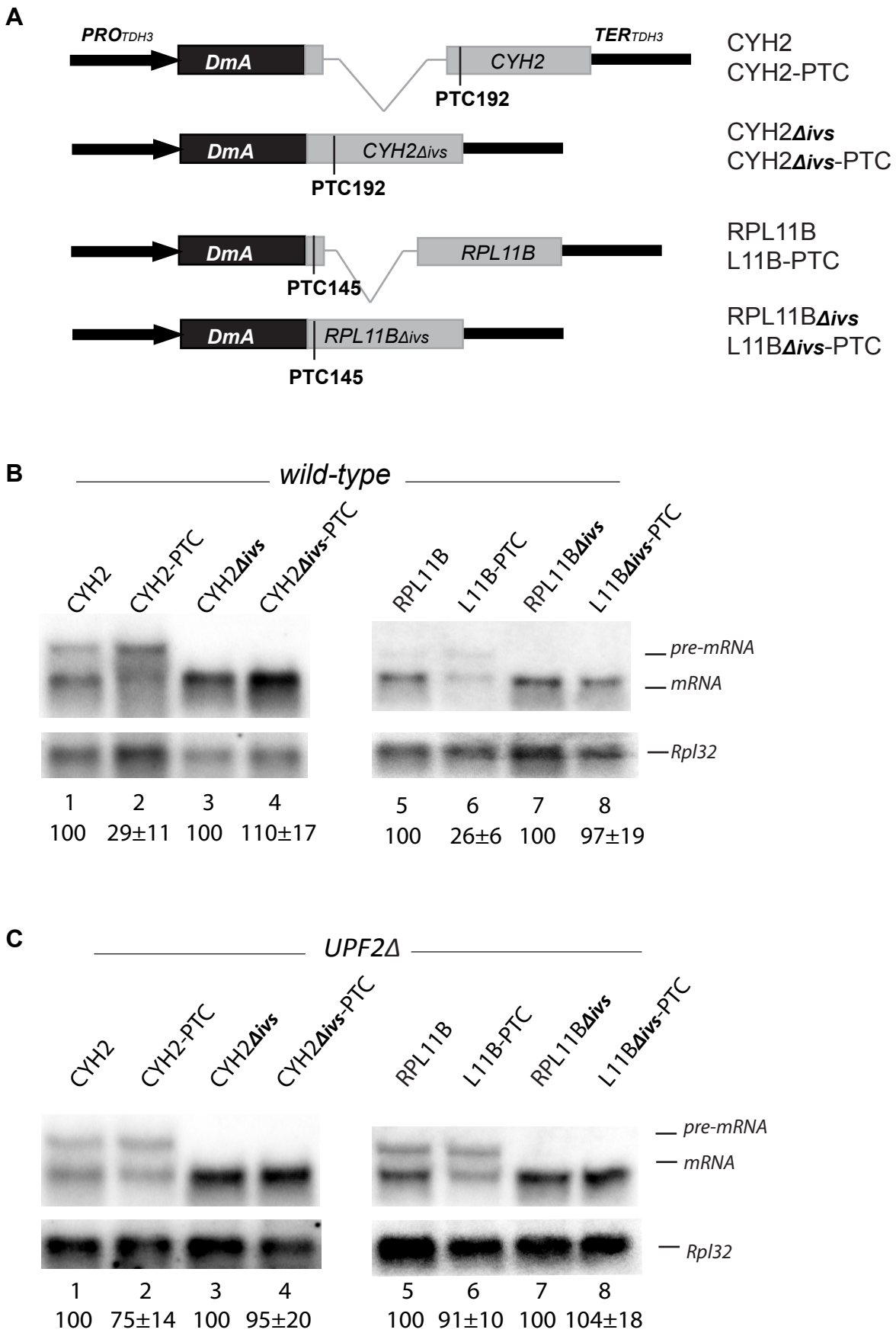
A
PROTDH3
DmA
CYH2
TERTDH3
PTC192
CYH2
CYH2-PTC
DmA
CYH2Δivs
PTC192
CYH2Δivs
CYH2Δivs-PTC
DmA
RPL11B
PTC145
RPL11B
L11B-PTC
DmA
RPL11BΔivs
PTC145
RPL11BΔivs
L11BΔivs-PTC
B
wild-type
CYH2
CYH2-PTC
CYH2Δivs
CYH2Δivs-PTC
RPL11B
L11B-PTC
RPL11BΔivs
L11BΔivs-PTC
pre-mRNA
mRNA
Rpl32
1 2 3 4
100 29±11 100 110±17
5 6 7 8
100 26±6 100 97±19
C
UPF2Δ
CYH2
CYH2-PTC
CYH2Δivs
CYH2Δivs-PTC
RPL11B
L11B-PTC
RPL11BΔivs
L11BΔivs-PTC
pre-mRNA
mRNA
Rpl32
1 2 3 4
100 75±14 100 95±20
5 6 7 8
100 91±10 100 104±18

A

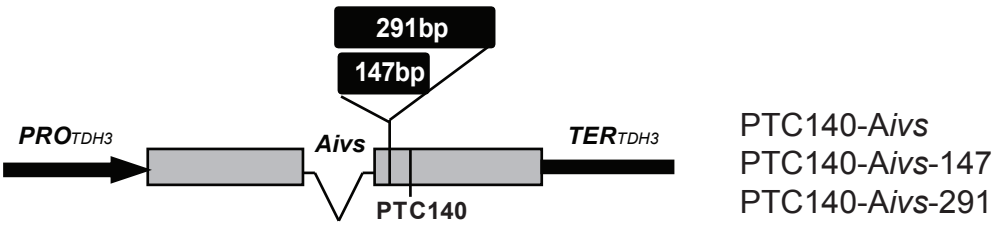
291bp
147bp
PROTDH3
Aivs
TERTDH3
PTC140
PTC140-Aivs
PTC140-Aivs-147
PTC140-Aivs-291

B

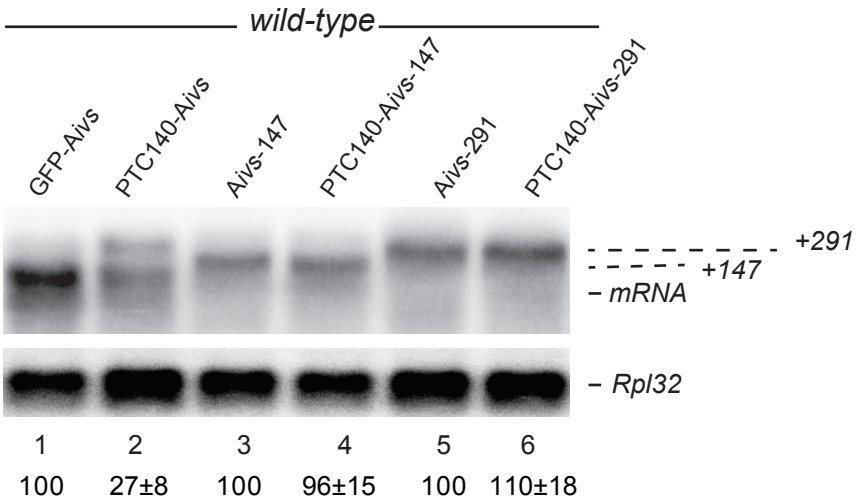
wild-type
GFP-Aivs
PTC140-Aivs
Aivs-147
PTC140-Aivs-147
Aivs-291
PTC140-Aivs-291
+291
+147
mRNA
Rpl32
1 2 3 4 5 6
100 27±8 100 96±15 100 110±18

C

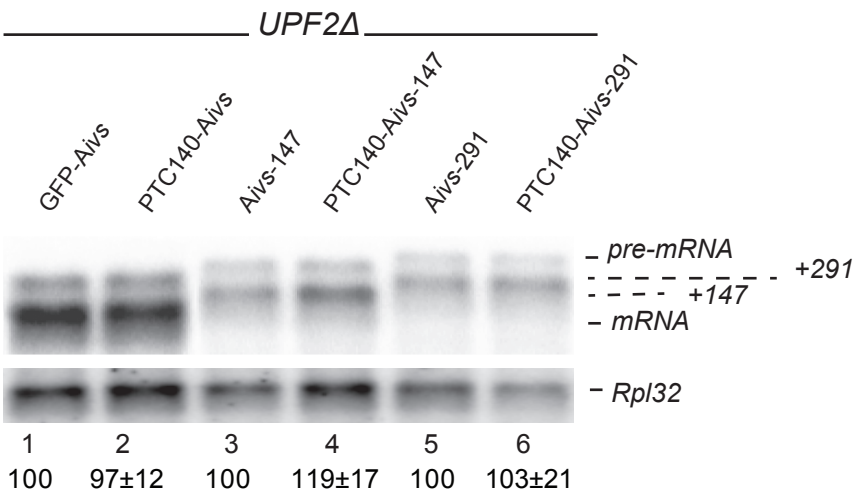
UPF2Δ
GFP-Aivs
PTC140-Aivs
Aivs-147
PTC140-Aivs-147
Aivs-291
PTC140-Aivs-291
pre-mRNA
+291
+147
mRNA
Rpl32
1 2 3 4 5 6
100 97±12 100 119±17 100 103±21

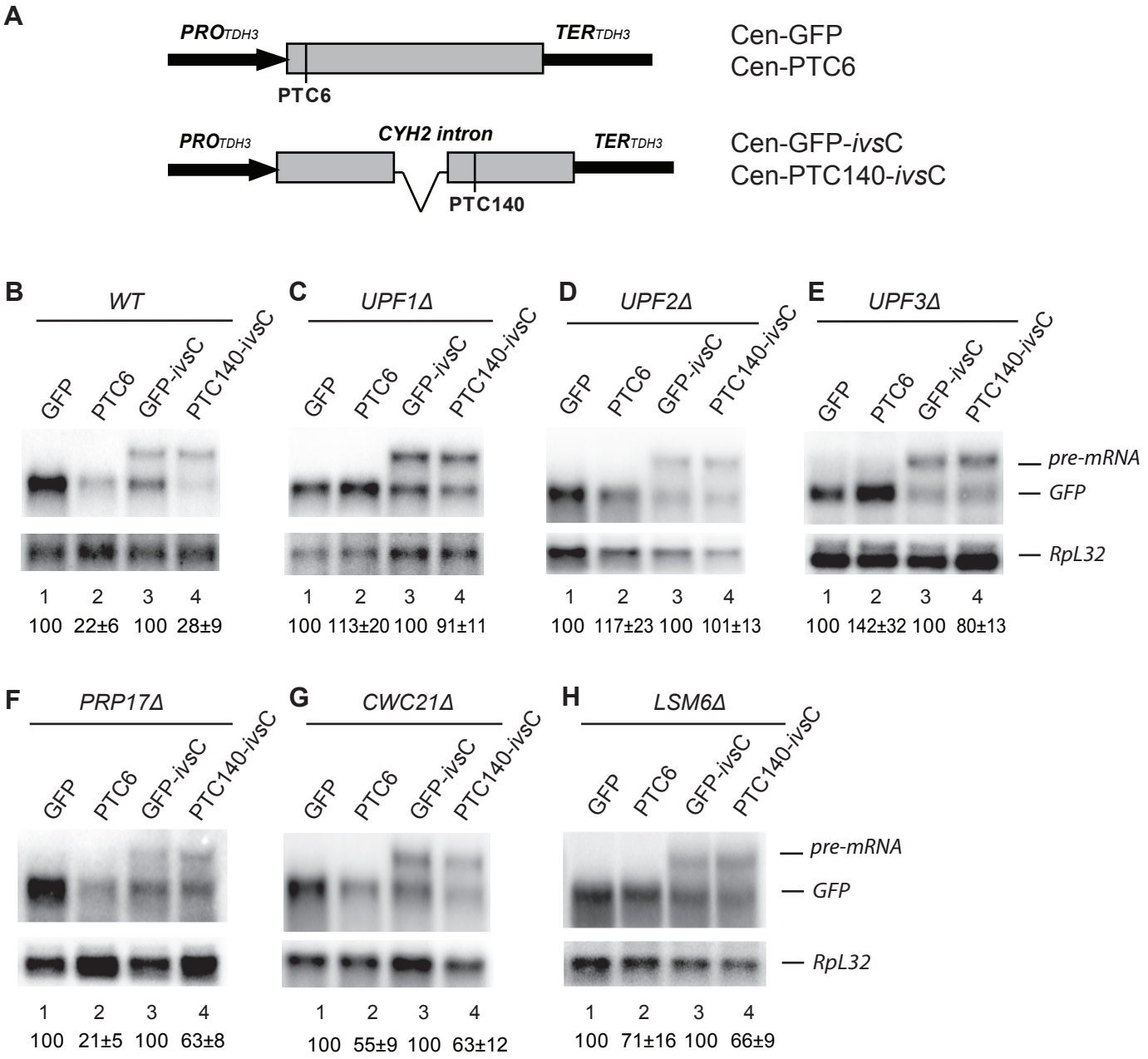
A
PROTDH3
TERTDH3
PTC6
Cen-GFP
Cen-PTC6
CYH2 intron
PTC140
Cen-GFP-ivsC
Cen-PTC140-ivsC
B
WT
C
UPF1Δ
D
UPF2Δ
E
UPF3Δ
GFP
PTC6
GFP-ivsC
PTC140-ivsC
pre-mRNA
GFP
RpL32
1 2 3 4
100 22±6 100 28±9
100 113±20 100 91±11
100 117±23 100 101±13
100 142±32 100 80±13
F
PRP17Δ
G
CWC21Δ
H
LSM6Δ
100 21±5 100 63±8
100 55±9 100 63±12
100 71±16 100 66±9

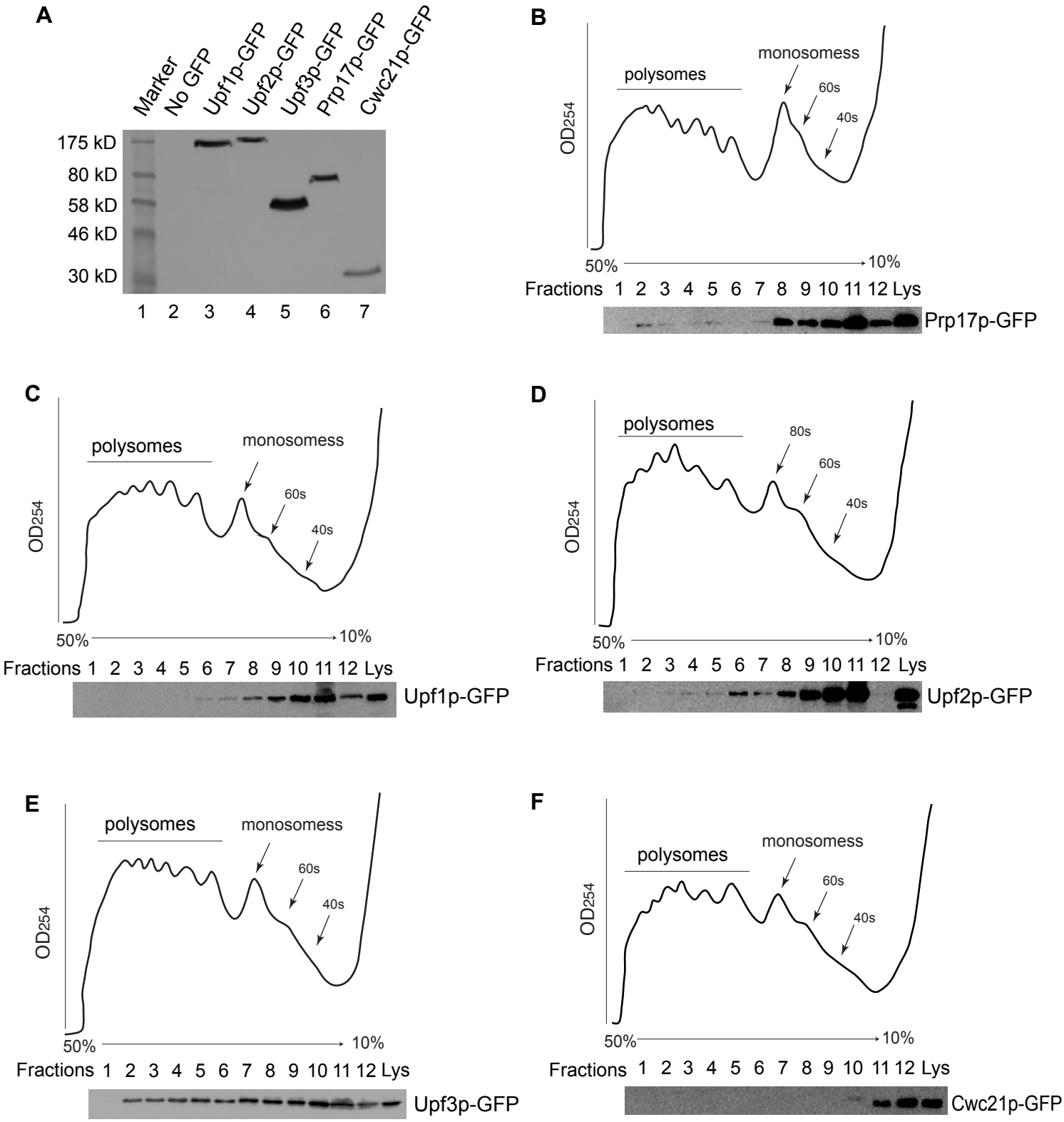
A
Marker
No GFP
Upf1p-GFP
Upf2p-GFP
Upf3p-GFP
Prp17p-GFP
Cwc21p-GFP
175 kD
80 kD
58 kD
46 kD
30 kD
1 2 3 4 5 6 7
B
polysomes
monosomess
60s
40s
OD254
50%
10%
Fractions 1 2 3 4 5 6 7 8 9 10 11 12 Lys
Prp17p-GFP
C
polysomes
monosomess
60s
40s
OD254
50%
10%
Fractions 1 2 3 4 5 6 7 8 9 10 11 12 Lys
Upf1p-GFP
D
polysomes
80s
60s
40s
OD254
50%
10%
Fractions 1 2 3 4 5 6 7 8 9 10 11 12 Lys
Upf2p-GFP
E
polysomes
monosomess
60s
40s
OD254
50%
10%
Fractions 1 2 3 4 5 6 7 8 9 10 11 12 Lys
Upf3p-GFP
F
polysomes
monosomess
60s
40s
OD254
50%
10%
Fractions 1 2 3 4 5 6 7 8 9 10 11 12 Lys
Cwc21p-GFP

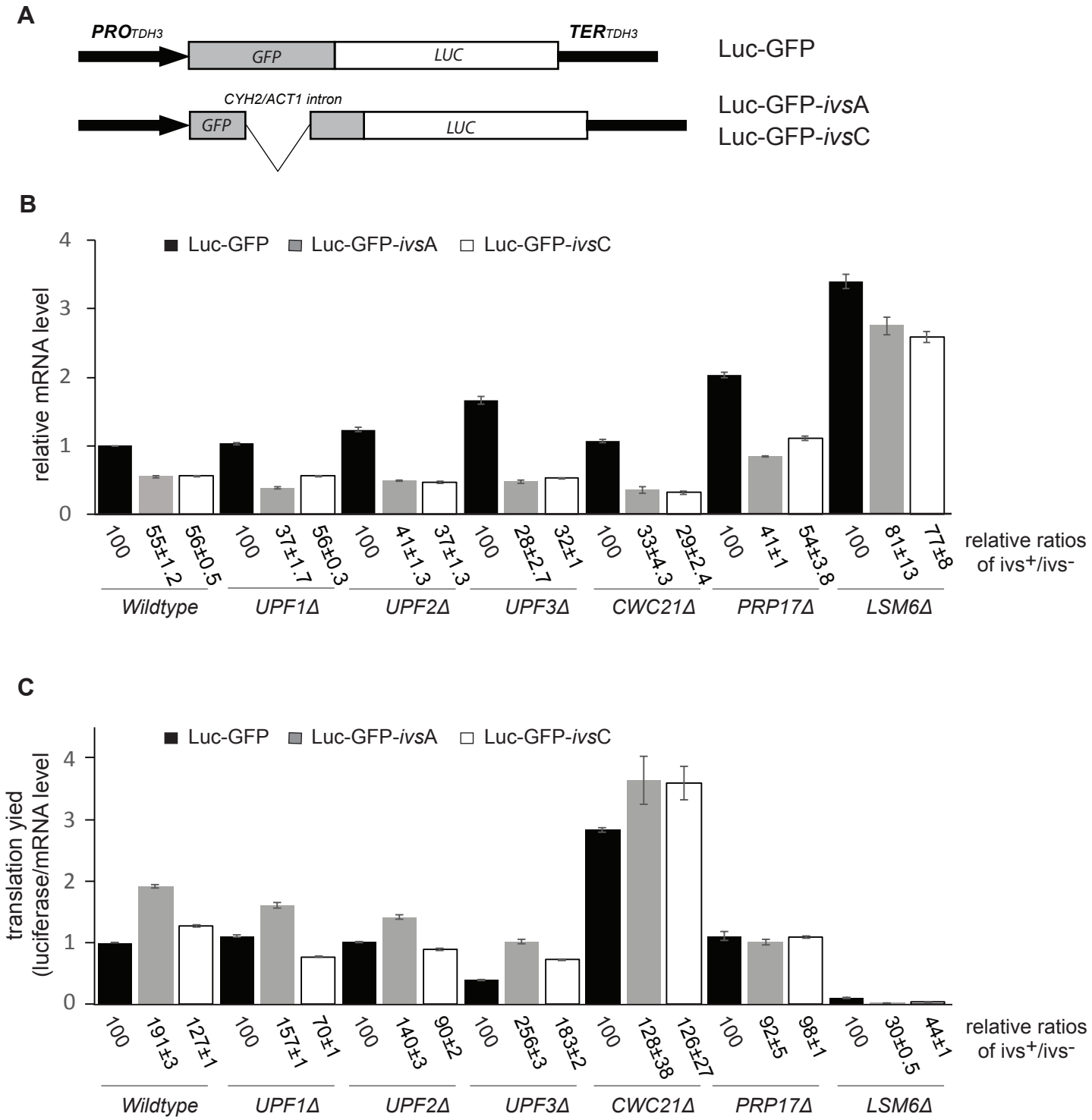
A
PROTDH3
TERTDH3
GFP
LUC
Luc-GFP
CYH2/ACT1 intron
GFP
LUC
Luc-GFP-ivsA
Luc-GFP-ivsC
B
Luc-GFP
Luc-GFP-ivsA
Luc-GFP-ivsC
relative mRNA level
0
1
2
3
4
100
55±1.2
56±0.5
100
37±1.7
56±0.3
100
41±1.3
37±1.3
100
28±2.7
32±1
100
33±4.3
29±2.4
100
41±1
54±3.8
100
81±13
77±8
relative ratios of ivs+/ivs-
Wildtype
UPF1Δ
UPF2Δ
UPF3Δ
CWC21Δ
PRP17Δ
LSM6Δ
C
Luc-GFP
Luc-GFP-ivsA
Luc-GFP-ivsC
translation yied (luciferase/mRNA level
0
1
2
3
4
100
191±3
127±1
100
157±1
70±1
100
140±3
90±2
100
256±3
183±2
100
128±38
126±27
100
92±5
98±1
100
30±0.5
44±1
relative ratios of ivs+/ivs-
Wildtype
UPF1Δ
UPF2Δ
UPF3Δ
CWC21Δ
PRP17Δ
LSM6Δ

Wen et al.

Supplementary information.

Three tables and one figure.

Supplementary Table 1. Strains used in this study

Strains name	genotype
W303a	*MATa ade2-1 trp1-1 can1-100 leu2-3,112 his3-11,15 ura3-1*
UPF1*Δ*	*MATa ade2-1 trp1-1 can1-100 leu2-3,112 his3-11,15 ura3-1 upf1::HIS3*
UPF2*Δ*	*MATa ade2-1 trp1-1 can1-100 leu2-3,112 his3-11,15 ura3-1 upf2::HIS3*
BY4742	*MATα his3Δ1 leu2Δ0 lys2Δ0 ura3Δ0*
CWC21*Δ*	*MATa ade2-1 trp1-1 can1-100 leu2-3,112 his3-11,15 ura3-1 cwc21::KanMX6*
PRP17*Δ*	*MATa ade2-1 trp1-1 can1-100 leu2-3,112 his3-11,15 ura3-1 prp17::KanMX6*
UPF1-GFP	*MATa his3Δ1 leu2Δ0 met15Δ0 ura3Δ0 upf1::upf1-GFP-HIS3*
UPF2-GFP	*MATa his3Δ1 leu2Δ0 met15Δ0 ura3Δ0 upf2::ufp2-GFP-HIS3*
UPF3-GFP	*MATa his3Δ1 leu2Δ0 met15Δ0 ura3Δ0 upf3::ufp3-GFP-HIS3*
PRP17-GFP	*MATa his3Δ1 leu2Δ0 met15Δ0 ura3Δ0 prp17::prp17-GFP-HIS3*
CWC21-GFP	*MATa his3Δ1 leu2Δ0 met15Δ0 ura3Δ0 cwc21::cwc21-GFP-HIS3*
BY4741	*MATa his3Δ1 leu2Δ0 met15Δ0 ura3Δ0*

Supplementary Table 2. Primers in this study

Primer names	DNA sequence (5’ to 3’)
Act.ivs.for	GTATGTTCTAGCGCTTGCAC
Act.ivs.rev	CTAAACATATAATATAGCAAC
Cyh.ivs.for	GTATGTAGTTCCATTTGGAAG
Cyh.ivs.rev	CTGTACAAAAAAAATATTGTAATG
Uivs.full.fow	GTATGTCTAAAGTTATGGCCACGTTTCAAATGCGTG CTTTTTTTTTAAAACTTATGCTCTTATTTACTAACAA AATCAACATGCTATTGAACTAG
Uivs.full.rev	CTAGTTCAATAGCATGTTGATTTTGTTAGTAAATAAG AGCATAAGTTTTAAAAAAAAAGCACGCATTTGAAAC

	GTGGCCATAACTTTAGACATAC
ScL11b.P145.fow	CCCCGGATCCTCCACTGAA**TAA**ACTGTTCAATCTG
ScL11b.wt.fow	CCCCGGATCCTCCACTGAATTAACTGTTCAATCTG
ScL11b.rev	CCCCGTCGACTTAAAATTTAGCAAATTGCTTGTTGG
Sccyh2.wt.fow	CCCCGGATCCCCTTCCAGATTCACTAAGACTAGAAA GCAC
Sccyh2.rev	CCCCGTCGACTTAAGCGATCAATTCAACAACACC
Sccyh2.P192.rev	GTTGACCACC**TTA**CATACCTCTACCACCG
Sccyh2.P192.fow	GGTAGAGGTATG**TAA**GGTGGTCAACATCACCACAG
Sc.l32.fow	TACCTCACCCAAAGATTGTC
Sc.l32.rev	GGTTTCCAAATCCTTAACG
Adh.Bgl.fow	AGTCCAGATCTATGTCGTTTACTTTGACCAACAAG
Adh.Bam.rev	CTTTGAAGATAAAGAGGATCCAATGTTGCAGATGAT
F.Luc.fow	CTTGAGCCTAGGTACCCATACGATGTTCCTGA
F.Luc147.rev	TTTGTACCTAGGCTCGACCAGGATGGGCAC
F.Luc291.rev	TTGGTTCCTAGGGGTCAGGGTGGTCACGAG
GFP.Q.fow	GAGTTGTCCCAATTCTTGTT
GFP.Qs.rev	TTGACTTCAGCACGTGTCTT

Supplementary Table 3. Non-essential splicing mutants and proteins predicted to interact with known NMD factors

BY4742 strains with deletions	protein name
YHR086W	Nam8p
YBR119W	Mud1p
YPL213W	Lea1p
YIR009W	Msl1p
YHR156C	Snu40p
YOR308C	Snu66p
YNL147W	LSm7p
YDR378C	LSm6p

YGL174W	Bud13p
YLR016C	Pml1p
YJR050W	Isy1p
YJK138C	Tif2p
YDL160C	Dhh1p
YDR206W	Ebs1p
YPR057W	Brr1p
YGR129W	Syf2p
YPR101W	Snt309p
YBR188C	Ntc20p
YBR065C	Ecm2p
YDR163W	Cwc15p
YPR152C	Urn1p
YDR482C	Cwc21p
YGR006W	Prp18p
YMR125W	Sto1p
YPL178W	Cbc2p
YMR080C	Upf1p
YHR072C	Upf2p
YGR072W	Upf3p
YGL246W	Rai1p
YKR059W	Tif1p
YDR363W	Esc2p
YPL064C	Cwc27p
YDR364C	Prp17p

Supplementary figure legends

Supplementary Figure 1. Prp17p is required for splicing enhanced NMD in the Aivs reporter.

(A) Schematic maps of the NMD reporters used in the deletion mutants screening for novel NMD mutants. (B-E) RNA analysis carried out in different yeast strains by Northern blotting. The top panel shows the GFP mRNA transcripts, the bottom panel shows the normalization control *Rpl32B* mRNA. All of the experiments were repeated three times.

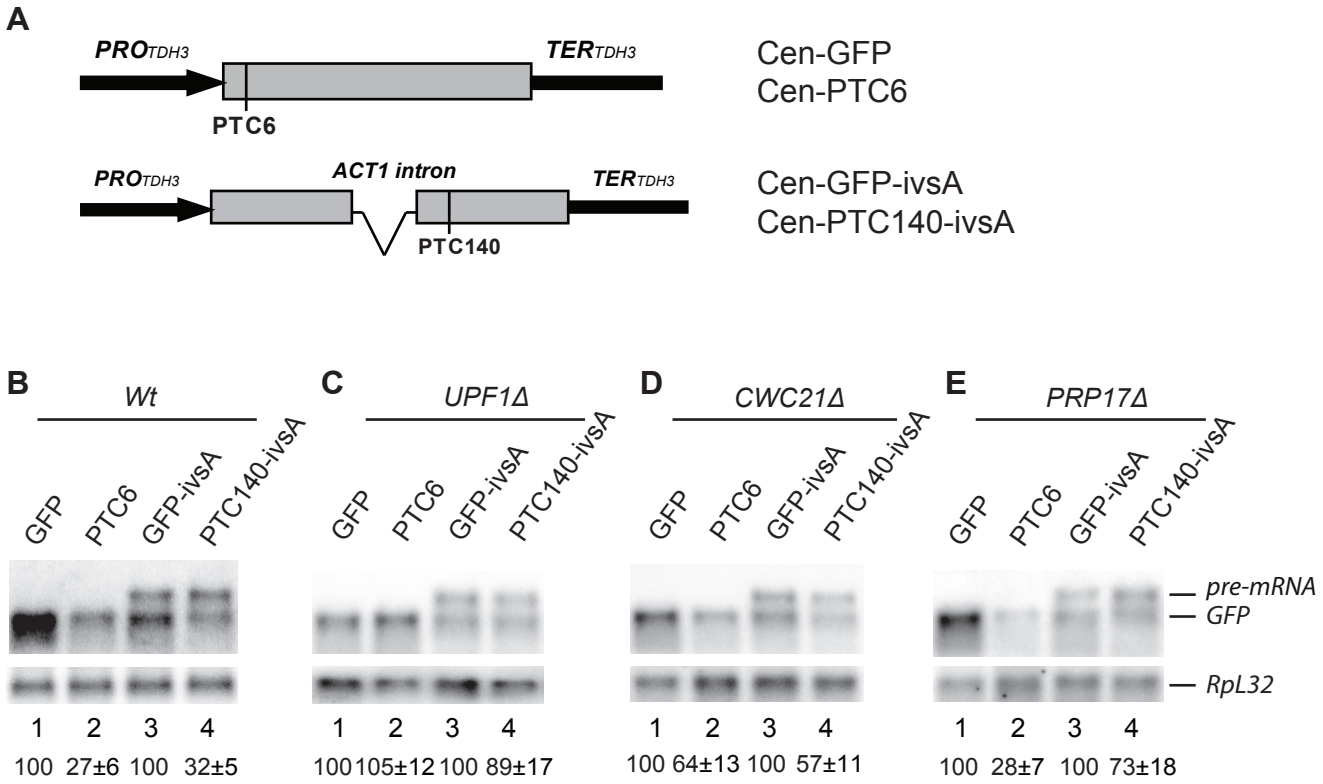
A
PROTDH3
TERTDH3
PTC6
Cen-GFP
Cen-PTC6
PROTDH3
ACT1 intron
TERTDH3
PTC140
Cen-GFP-ivsA
Cen-PTC140-ivsA
B
Wt
C
UPF1Δ
D
CWC21Δ
E
PRP17Δ
GFP
PTC6
GFP-ivsA
PTC140-ivsA
pre-mRNA
GFP
RpL32
1 2 3 4
100 27±6 100 32±5
1 2 3 4
100 105±12 100 89±17
1 2 3 4
100 64±13 100 57±11
1 2 3 4
100 28±7 100 73±18